



ISSN:1991-8178

## Australian Journal of Basic and Applied Sciences

Journal home page: www.ajbasweb.com



### Properties of N-Octadecane-Encapsulated Activated Carbon Nanocomposite for Energy Storage Medium: The Effect of Surface Area and Pore Structure

<sup>1</sup>Mohd Zobir Hussein, <sup>2</sup>Tumirah Khadiran, <sup>3</sup>Zulkarnain Zainal and <sup>4</sup>Rafeadah Rusli

<sup>1</sup>Material Synthesis and Characterization Laboratory (MSCL), Institute of Advanced Technology (ITMA), Universiti Putra Malaysia (UPM), 43400 Serdang, Selangor, Malaysia.

<sup>2</sup>Material Synthesis and Characterization Laboratory (MSCL), Institute of Advanced Technology (ITMA), Universiti Putra Malaysia (UPM), 43400 Serdang, Selangor, Malaysia.

<sup>3</sup>Material Synthesis and Characterization Laboratory (MSCL), Institute of Advanced Technology (ITMA), Universiti Putra Malaysia (UPM), 43400 Serdang, Selangor, Malaysia.

<sup>4</sup>Forest Product Division, Forest Research Institute of Malaysia (FRIM), 52100 Kepong, Selangor, Malaysia.

#### ARTICLE INFO

##### Article history:

Received 12 February 2015

Accepted 1 March 2015

Available online 28 March 2015

##### Keywords:

Activated carbon; peat soil; thermal energy storage; phase change material; n-octadecane

#### ABSTRACT

Shape-stabilized phase change materials (PCMs) composed of n-octadecane encapsulated into activated carbon (AC) micro- and meso-pores were prepared by direct impregnation method. Three types of ACs with different pore structures were used as frameworks, namely AC prepared from peat soil using phosphoric acid activation method (PSAC-C) and physical activation method (PSAC-P), and a commercial activated carbon (CAC). The results show that the phase change properties of the n-octadecane/AC PCM nanocomposite are governed by the pore structure-adsorption interaction of the n-octadecane on the AC. Generally, the specific surface area is the important parameter, which is directly proportional to the latent heat of fusion and encapsulation efficiency. Similarly, the encapsulation efficiency is directly proportional to the latent heat of fusion. This study shows that peat soil is a potential, cheap source for activated carbon which can be used as inorganic frameworks for the preparation of shape-stabilized phase change materials which can be designed by tuning the pore structures of the activated carbon.

© 2015 AENSI Publisher All rights reserved.

**To Cite This Article:** Mohd Zobir Hussein, Tumirah Khadiran, Zulkarnain Zainal and Rafeadah Rusli., Properties of N-Octadecane-Encapsulated Activated Carbon Nanocomposite for Energy Storage Medium: The Effect of Surface Area and Pore Structure. *Aust. J. Basic & Appl. Sci.*, 9(8): 82-88, 2015

#### INTRODUCTION

Thermal energy storage (TES) based on phase change materials (PCMs) is an advanced material, which can be used in improvement of efficient energy management and utilization. PCMs are more preferred to be used for heat storage medium due to their high energy storage density during their melting processes and narrow operating temperature range (Bo *et al.*, 2004; Xia *et al.*, 2010). PCM can be generally classified into two classes, namely organic (n-alkanes, fatty acid, ethylene glycol) and inorganic (salt hydrates) (Zalba *et al.*, 2003). Organic PCMs are widely used for TES medium, especially for energy conservation in buildings beside other applications such as solar energy systems, thermal insulation, textiles and transportation (Zhang *et al.*, 2012; Mondal 2008), as they have high thermal storage capacities and other properties such as good thermal stability and non-toxic (Zalba *et al.*, 2003; Tyagi *et al.*, 2011). However, organic PCMs suffered

with low thermal conductivity that causes supercooling and leakage problem during it melting state (Cheng *et al.*, 2010; Sari *et al.*, 2008). This will limit their application as energy storage material.

Many supporting materials were reported to be used to solve this problem like polymer-based materials. Recently, many researchers focusing on the use of inorganic-based materials such as expanded graphite (Zhengguo *et al.*, 2012), expanded perlite (Sari *et al.*, 2009), SiO<sub>2</sub> (Qian *et al.*, 2015), carbon nanotube (Yu *et al.*, 2014) and graphene oxide (Mehrali *et al.*, 2013), due to their high porosity and surface area. These properties are good to be used as supporting material which subsequently increased the thermal stability of PCM. However, most of inorganic-based materials are expensive and difficult to synthesise, especially expanded graphite, graphene oxide and carbon nanotube, and therefore are not economical to be used for building or other applications.

**Corresponding Author:** Mohd Zobir Hussein, Material Synthesis and Characterization Laboratory (MSCL), Institute of Advanced Technology (ITMA), Universiti Putra Malaysia (UPM), 43400 Serdang, Selangor, Malaysia.  
Tel: 603-89468092; Fax: 603-89467006; E-mail: mzobir@upm.edu.my

Recently, activated carbon has drawn great attention for being able to provide PCM with both good thermal conductivity and form-stability (Chen *et al.*, 2012; Feng *et al.*, 2011). Wang *et al.* (2012) reported that the porous networks of AC play an important role in tailoring the properties of shape-stabilized PCM. It was suggested that AC pores with micro- and nano-meter sized exhibit the same properties of shape-stabilization ability, in term of minimize the enthalpy loss. Unfortunately, the pore structure of AC with similar pore size distribution, network-inner-connection and the geometrical shape of AC are difficult to obtain. The pore structures, namely BET specific surface area, total pore diameter and average pore volume of AC depend on several factors, especially the type of carbon precursor and activation method used (Gonzalez-Garia *et al.*, 2013). Therefore, the energy storage ability of PCM in the pores of AC is complicated and difficult to study. This encourages us to develop AC from peat soil, which is abundant and relatively cheap. The emphasis of this study was to optimize the processes to tailor the low cost AC with excellent pore structures and compare their performance as an inorganic framework with a commercial activated carbon (CAC).

In this work, we study the effect of pore structures; particularly BET specific surface area, total pore diameter and average pore volume of the ACs on the energy storage properties of shape-stabilized PCM. In this work, n-octadecane was used as the PCM, and it was encapsulated into the pores of 3 different ACs with different pore structure properties, which act as the inorganic frameworks for the formation of shape-stabilized PCMs.

### **Experimental:**

#### **Materials:**

Peat soil was collected from Sabak Bernam, Malaysia. The peat soil sample was oven-dried at 60 °C for 48 h, powdered, sieved through a 0.5 mm sieve, and kept in a desiccator to be used as a precursor for AC preparation. Commercial activated carbon (CAC), and analytical reagents grade chemicals purchased from Sigma-Aldrich were used in this study.

#### **Preparation of Peat Soil Activated Carbon:**

Phosphoric acid ( $H_3PO_4$ ) was used as the activation agent for preparation of peat soil activated carbon (PSAC-C) using chemical activation method. 5 g of dried peat soil was impregnated with a 50 mL solution of 30%  $H_3PO_4$  and left at 70 °C in an oil bath shaker (100 rpm) until all the excess water was evaporated. The sample was then oven-dried at 120 °C, overnight. Then the sample was carbonized at 500 °C for 3 h in a tubular electric furnace under an inert flow of nitrogen ( $N_2$ ) gas with a flow rate of 100  $cm^3\ min^{-1}$ . The heating rate of 10 °C  $min^{-1}$  was used throughout the carbonization process. The

resulting AC was cooled at room temperature and refluxed with water for 24 h, followed by washing with distilled water. The obtained AC was then oven-dried at  $102 \pm 3$  °C, overnight. The dried AC sample, labelled as PSAC-C was transferred into a sample bottle and kept in a desiccator for further use and characterizations.

AC was also prepared using physical activation technique. About 5 g of dried peat soil sample was placed in a porcelain cup with lid and carbonized at 800 °C for 7 h in a box furnace. The heating rate of 5 °C  $min^{-1}$  was used in this study. The resulting carbon was activated under atmospheric pressure at 500 °C. The obtained AC (PSAC-P) was transferred into a sample bottle and kept in a desiccator for further use and characterizations.

#### **Preparation of shape-stabilized n-octadecane/activated carbon nanocomposite:**

The n-octadecane/AC (0.9:1) nanocomposites were prepared by a simple impregnation method. The melted n-octadecane was dissolved in 30 mL absolute ethanol. PSAC-C or PSAC-P or CAC was added into the n-octadecane solution and the solution was then stirred at 600 rpm for 4 h. The mixture was then oven-dried at 80 °C for 48 h or until all the excess ethanol was evaporated. The preparation of n-octadecane/AC nanocomposites were repeated for two times.

#### **Characterization methods:**

The pore structures (BET specific surface area, total pore volume and average pore diameter) of PSAC-P, PSAC-C, CAC, and their nanocomposites, n-octadecane/PSAC-P nanocomposite, n-octadecane/PSAC-C nanocomposite and n-octadecane/CAC nanocomposite were determined by the  $N_2$  gas adsorption-desorption method at 77 K, using an Accelerated Surface Area and Porosimeter (ASAP) (Micromeretic, 2000). This instrument is one of the powerful tools to determine whether PCM was successfully infiltrated into the pores of AC or only existed on the surface of AC. The BET specific surface area and pore size distribution of the samples were determined using the Brunauer-Emmet-Teller (BET) and Barrett-Joyner-Halenda (BJH) equations, respectively.

The energy storage properties of n-octadecane/AC nanocomposites, such as melting temperature, freezing temperature and latent heat were measured by a differential scanning calorimetry (DSC) (822e, Mettler Toledo) equipped with a refrigerated cooling system. The measurements were performed at a heating rate of 10 °C  $min^{-1}$  at -10 to 70 °C for heating cycle stage and 70 to -20 °C for the freezing stage under a constant  $N_2$  atmosphere at a flow rate of 60  $mL\ min^{-1}$ . The n-octadecane content in the n-octadecane/AC nanocomposites was determined using the following equation:

PCM content in nanocomposite (wt. %) =  $(\Delta H_m / \Delta H_{PCM}) \times 100$  (1)

where  $\Delta H_m$  is enthalpy of melting for the analysed n-octadecane/AC nanocomposites ( $Jg^{-1}$ ) and  $\Delta H_{PCM}$  is the enthalpy of melting for the pure n-octadecane ( $Jg^{-1}$ ) (Alkan *et al.*, 2011).

## RESULTS AND DISCUSSION

### Pore structures of activated carbon:

The pore structure of AC depends on the activation method used and the type of carbon precursor. AC with different pore structures has

significant effect on the stabilization ability and energy storage capability of PCM. The properties of the AC used in this study are summarized in Table 1, which shows the properties of AC before and after they were infiltrated with n-octadecane. Fig. 1 and Fig. 2 illustrate the  $N_2$  adsorption-desorption isotherms of PSAC-P, PSAC-C, CAC and their nanocomposites, respectively. Fig. 3 illustrates the BJH desorption pore size distribution of PSAC-C, PSAC-P and CAC, while Fig. 4 shows the BJH desorption pore size distribution of n-octadecane/PSAC-C, n-octadecane/PSAC-P and n-octadecane/CAC nanocomposites, respectively.

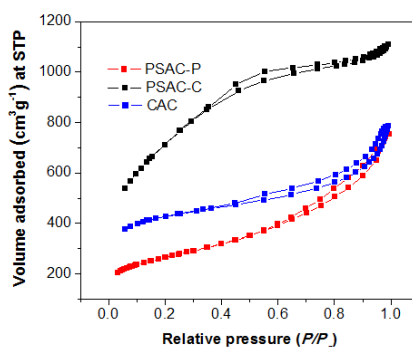


**Fig. 1:**  $N_2$  adsorption-desorption isotherms of ACs; PSAC-P, PSAC-C and CAC.

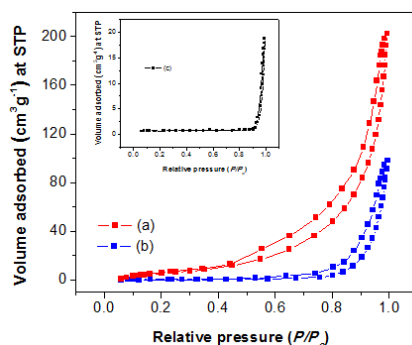


**Fig. 2:**  $N_2$  adsorption-desorption isotherm of (a) n-octadecane/PSAC-P nanocomposite, (b) n-octadecane/CAC nanocomposite and (c) n-octadecane/PSAC-C nanocomposite (inset).

**Table 1:** Characteristics of the ACs and their n-octadecane-encapsulated AC nanocomposites.

Sample	BET specific surface area ( $m^2/g$ )	Pore volume ( $cc/g$ )	Pore width ( $\text{\AA}$ )
PSAC-C	1974	1.41	32
PSAC-P	893	0.88	22
CAC	1468	0.80	58
n-octadecane/PSAC-C	1	0.02	451
n-octadecane/PSAC-P	12	0.03	56
n-octadecane/CAC	1	0.03	425

As can be observed in Fig. 1, the PSAC-C exhibits a combination of Type I and Type II adsorption-desorption isotherms according to the IUPAC classification (Sing *et al.*, 1985), indicating the simultaneous presence of micro- and meso-pores. A similar property is also observed for the isotherms of PSAC-P and CAC. As shown in Fig. 1 the isotherms of PSAC-P, PSAC-C and CAC exhibited a well-defined plateau with open hysteresis loops,

extending to a relative pressure of  $P/P_0 \approx 1.0$ , indicating a mesopore-rich texture. The extrapolation of isotherm knee for all the AC samples clearly shows the microporous-rich nature of all the ACs in the order of PSAC-C > CAC > PSAC-P.

The  $N_2$  adsorption-desorption isotherm and pore size distribution of n-octadecane/PSAC-P nanocomposite, n-octadecane/PSAC-C nanocomposite and n-octadecane/CAC

nanocomposite are shown in Fig. 2. The purpose of this study is to prove that n-octadecane was successfully infiltrated into the pores of ACs. Fig. 2 shows that  $N_2$  adsorption-desorption isotherm of all the nanocomposites is of Type IV, indicating that the resulting nanocomposites has low adsorption affinity.

The adsorption affinity decreased in the order of; n-octadecane/PSAC-P > n-octadecane/CAC > n-octadecane/PSAC-C. This agrees nicely with the microporous-rich nature of the ACs. As expected, this is due to the microporous nature of the ACs that was occupied by n-octadecane.

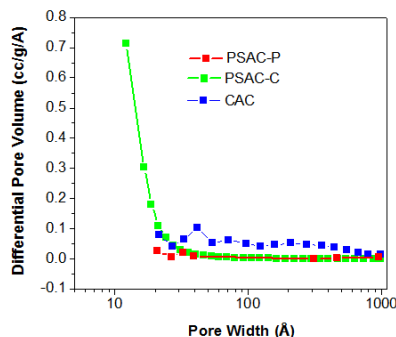


**Fig. 3:** BJH desorption pore size distribution of ACs; PSAC-P, PSAC-C and CAC.

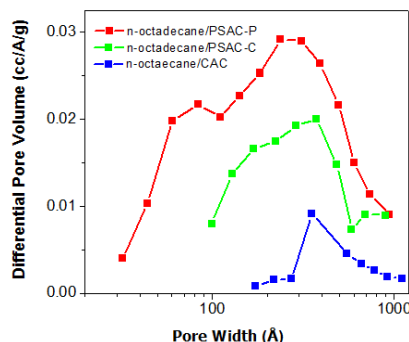


**Fig. 4:** BJH desorption pore size distribution of n-octadecane/PSAC-C, n-octadecane/PSAC-P and n-octadecane/CAC nanocomposites.

As can be observed in Table 1 and Fig. 3, the PSAC-C has a largest BET specific surface area, followed by CAC and PSAC-P. BET specific surface area, total pore volume and average pore diameter of PSAC-C are  $1974 \text{ m}^2/\text{g}$ ,  $1.41 \text{ cc/g}$  and  $32 \text{ \AA}$ , respectively. However, the BET specific surface area and total pore volume of n-octadecane/PSAC-C nanocomposite was decreased to  $1 \text{ m}^2/\text{g}$  and  $0.02 \text{ cc/g}$ , respectively, as a result of n-octadecane encapsulation. As expected, the average pore diameter of n-octadecane/PSAC-C nanocomposite is higher than the average pore diameter of the PSAC-C, which is  $451 \text{ \AA}$  (Fig. 4) indicating that all the micropores and some of the mesopores of ACs were filled up by n-octadecane. This clearly indicates that n-octadecane was fully infiltrated into the porous network of the ACs. A similar trend was also observed for n-octadecane/PSAC-P and n-octadecane/CAC nanocomposites.

Fig. 4 shows that PSAC-P has less ability to encapsulate n-octadecane compared to PSAC-C and CAC. The mesopores are still available even after it was infiltrated with n-octadecane. It seems that the pores of PSAC-P has less capillary force and

hydrogen bonding, thus lead to lower content of n-octadecane in the n-octadecane/PSAC-P nanocomposite. This presumably, due to the surface chemistry of the PSAC-P which contains less surface functional groups.

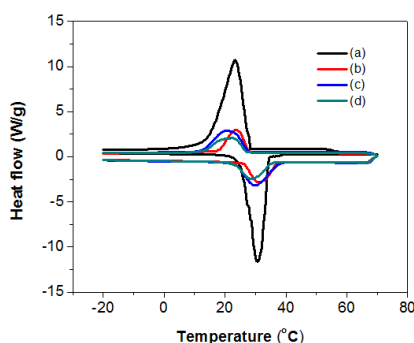
#### **Energy storage properties of n-octadecane/AC nanocomposites:**

Fig. 5 shows the DSC thermograms of pure n-octadecane and the three nanocomposites PCMs which were prepared using the 3 types of the ACs. In general, the melting and freezing temperatures of the nanocomposite PCMs decreases only slightly compared to that of pure n-octadecane (Fig. 5). The melting and freezing temperature of nanocomposite PCMs decreases in the order of n-octadecane/PSAC-C > n-octadecane/PSAC-P > n-octadecane/CAC nanocomposites. The shift of the melting peak is an indication of the strength of the interactions between the n-octadecane and the pores of the ACs. For strong interaction between PCMs and inorganic frameworks, the melting peak of PCMs will be shifted, while a weak interaction will lead to a

decrease in phase change temperature (Zhang *et al.*, 2007; Radhakrishnan *et al.*, 1999).

Table 2 shows the latent heat of fusion of the nanocomposite PCMs. Fig. 6a illustrated the BET specific surface area ( $\text{m}^2\text{g}^{-1}$ ) versus encapsulation efficiency (%) and latent heat of fusion ( $\text{Jg}^{-1}$ ), while Fig. 6b illustrated the encapsulation efficiency (%) versus latent heat of fusion ( $\text{Jg}^{-1}$ ). It is clear that the latent heat of fusion of the nanocomposite PCMs and encapsulation efficiency increased as the BET specific surface area of the AC materials increased. The latent heat of fusion is proportional to the

encapsulation efficiency. However, the decrease of the latent heat of the nanocomposite PCMs cannot be attributed to the BET specific surface area of the ACs only. Other factor that leads to the loss of the latent heat is due to the interactions between n-octadecane and AC materials. The strong interaction could hindered the n-octadecane from crystallizing, thus reduce the latent heat value of the nanocomposite PCMs. As shown in Table 2, the encapsulation efficiency of n-octadecane is also decreased as the porosity of the AC materials was decreased.



**Fig. 5:** DSC thermograms of (a) pure n-octadecane and shape-stabilized n-octadecane with different pore structures of ACs: (b) n-octadecane/PSAC-P, (c) n-octadecane/PSAC-C and (d) n-octadecane/CAC.

**Table 2:** Latent heat of fusion and encapsulation efficiency.

Samples	Latent heat of fusion ( $\text{Jg}^{-1}$ )	Encapsulation efficiency (%)
Pure n-octadecane	240.6	-
n-octadecane/PSAC-C	107.2	44.3
n-octadecane/PSAC-P	95.4	41.4
n-octadecane/CAC	101.3	42.5

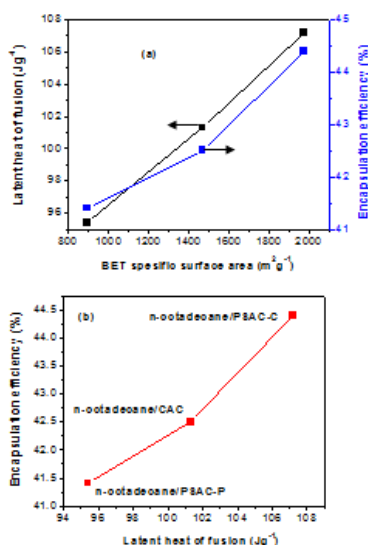


**Fig. 6:** Plot of (a) BET specific surface area ( $\text{m}^2\text{g}^{-1}$ ) versus encapsulation efficiency (%) and latent heat of fusion ( $\text{Jg}^{-1}$ ) and (b) encapsulation efficiency (%) versus latent heat of fusion ( $\text{Jg}^{-1}$ ).

### Conclusion:

Three types of n-octadecane encapsulated into pores framework of ACs for the formation of shape-stabilized PCMs/AC nanocomposite were prepared

by a simple one-step impregnation method using PSAC-C, PSAC-P and CAC as the supporting materials. The n-octadecane was used as a PCM to store energy, while PSAC-C, PSAC-P and CAC were

used as inorganic supporting materials or frameworks. The effect of the pore structure and the supporting material interaction on the phase change behavior of n-octadecane was studied. DSC results show that shape-stabilized n-octadecane with PSAC-C offering superior performance over the other two ACs. Based on the results obtained, this study suggests that different pore structures of inorganic supporting materials could give TES materials with different properties. The proper control of the pore structure of the inorganic supporting materials could be used to tailor the performance of TES material-based PCM. The findings from this study suggested that the energy storage properties of the shape-stabilized PCM could be design using different pore texture of AC, which can be tailor-made by controlling the parameters used during the activation process, such as holding time, carbonization temperature, and the type of activation agent. Generally, the specific surface area is the important parameter, which is directly proportional to the latent heat of fusion and encapsulation efficiency. Similarly, the encapsulation efficiency is directly proportional to the latent heat of fusion. This study showed that peat soil is a potential source of cheap activated carbon which can be used as inorganic frameworks for the preparation of shape-stabilized phase change materials.

#### ACKNOWLEDGEMENTS

This work was supported by the Ministry of Higher Education of Malaysia (MOHE), under grant no. FRGS/1/11/SG/UPM/01/2, and the JPA scholarship for Doctoral Program for TK is gratefully acknowledged.

#### REFERENCES

- Alkan, C., A. Sari and A. Karaipekli, 2011. Preparation, thermal properties and thermal reliability of microencapsulated n-eicosane as novel phase change material for thermal energy storage. *Energy Conversion & Management*, 52: 687-692.
- Bo, H., E.M. Gustafsson and F. Setterwall., 2004. Tetradecane and hexadecane binary mixtures as phase change materials (PCMs) for cool storage in district cooling systems. *Energy*, 29: 1785-1804.
- Chen, Z., F. Shan., L. Cao and G. Fang., 2012. Synthesis and thermal properties of shape-stabilized lauric acid/activated carbon composites as phase change materials for thermal energy storage. *Solar Energy Material and Solar Cells*, 102: 131-136.
- Cheng, W.I., R.M. Zhang, K. Xie, N. Liu and J. Wang, 2010. Heat conduction enhanced shape-stabilized paraffin/HDPE composite PCMs by graphite addition: preparation and thermal properties. *Solar Energy Material and Solar Cells*, 94: 1636-1642.
- Feng, L., L. Zheng., H. Yang., Y. Guo, W. Li and X. Li, 2011. Preparation and characterization of polyethylene glycol/activated carbon composites as shape-stabilized phase change materials. *Solar Energy Materials and Solar Cells*, 95: 644-650.
- Gonzalez-Garia, P., T.A. Centeno, E. Urones-Garrote, D. Avila-Brand and S. Otero-Diaz, 2013. Microstructure and surface properties of lignocellulosic-based activated carbons. *Applied Surface Science*, 265: 731-737.
- Mehrali, M., S.T. Latibari, M. Mehrali, H.S. Cornelis Metselaar and M. Silakhori, 2013. Shape-stabilized phase change materials with high thermal conductivity based on paraffin/graphene oxide composite. *Energy Conversion and Management*, 275-282.
- Mondal, S., 2008. Phase change materials for smart textiles – an overview. *Applied Thermal Engineering*, 28: 1536-1550.
- Qian, T., L. Jinhong, M. Hongwen and J. Yang, 2015. The preparation of a green shape-stabilized composite phase change material of polyethylene glycol/SiO<sub>2</sub> with enhanced thermal performance based on oil shale ash via temperature-assisted sol-gel method. *Solar Energy materials and Solar cells*, 132: 29-39.
- Radhakrishnan, R., K.E. Gubbins, A. Watanabe and K. Kaneko, 1999. Freezing of simple fluids in microporous activated carbon fibers: comparison of simulation and experiment. *Journal of Chemical Physics*, 111: 9058-9067.
- Sari, A., C. Alkan, A. Karaipekli and A. Oenal, 2008. Preparation, characterization and thermal properties of styrene maleic anhydride copolymer (SMA)/fatty acid composites as form stable phase change materials. *Energy Conversion and Management*, 49: 373-380.
- Sari, A., A. Karaipekli and C. Alkan, 2009. Preparation, characterization and thermal properties of lauric acid/expanded perlite as novel form-stable composite phase change material. *Chemical Engineering Journal*, 155: 899-904.
- Sing, K.S.W., D.H. Everett and R.A.W. Haul, 1985. Reporting physisorption data for gas/solid systems with special reference to the determination of surface area and porosity. *Pure Applied Chemistry*, 57: 603-619.
- Tyagi, V.V., S.C. Kaushik, S.K. Tyagi and T. Akiyama. Development of phase change materials based microencapsulated technology for buildings: a review. *Renewable Sustainable Energy Review*, 15: 1373-1391.
- Xia, L., P. Zhang and R.Z. Wang, 2010. Numerical heat transfer analysis of the packed bed latent heat storage system based on effective packed bed model. *Energy*, 35: 2022-2032.

Zalba, B., J.M. Marin, L.F. Cabeza and L. Mehling, 2003. Review on thermal energy storage with phase change: materials, heat transfer analysis and applications. *Applied Thermal Energy*, 23: 251-283.

Zhang, Z., N. Zhang, J. Peng, X. Fang, X. Gao and Y. Fang, 2012. Preparation and thermal energy storage properties of paraffin/expanded graphite composite phase change material. *Applied Energy*, 91: 426-431.

Zhang, D., S. Tian and D. Xiao, 2007. Experimental study on the phase change behavior of phase change material confined in pores. *Solar Energy*, 81: 653-660.

Zhengguo, Z., Z. Ni and P. Jing, 2012. Preparation and thermal energy storage properties of paraffin/expanded graphite composite phase change material. *Applied Energy*, 91(1): 426-431.